The Journal of Immunology

IL-1 Induces Proinflammatory Leukocyte Infiltration and Regulates Fibroblast Phenotype in the Infarcted Myocardium

Amit Saxena, Wei Chen, Ya Su, Vikrant Rai, Olisambu U. Uche, Na Li and Nikolaos G. Frangogiannis

J Immunol 2013; 191:4838-4848; Prepublished online 27 September 2013;
doi: 10.4049/jimmunol.1300725
http://www.jimmunol.org/content/191/9/4838

The Journal of Immunology is published twice each month by
The American Association of Immunologists, Inc.,
1451 Rockville Pike, Suite 650, Rockville, MD 20852

Print ISSN: 0022-1767 Online ISSN: 1550-6606.

IL-1 Induces Proinflammatory Leukocyte Infiltration and Regulates Fibroblast Phenotype in the Infarcted Myocardium

Amit Saxena,* Wei Chen,* Ya Su,* Vikrant Rai,* Olisambu U. Uche,† Na Li,* and Nikolaos G. Frangogiannis*,†

In the infarcted myocardium, activation of the inflammatory cascade clears the wound from dead cells, whereas stimulating matrix degradation and chamber dilation, thus contributing to the development of heart failure. IL-1 is critically involved in the postinfarction inflammatory reaction and mediates adverse dilative remodeling. We hypothesized that IL-1 may regulate postinfarction repair and remodeling through cell-specific actions on leukocytes and fibroblasts. Flow cytometry demonstrated that in mouse infarcts, early recruitment of proinflammatory Ly6C^{hi} cells expressing IL-1R1, the signaling receptor for IL-1, was followed by infiltration with cells expressing the decoy receptor, IL-1R2. Increased expression of IL-1R2 may serve to terminate IL-1–driven inflammation after infarction. Loss of IL-1 signaling in IL-1R1 null mice globally attenuated leukocyte recruitment, reducing the number of infiltrating Ly6C^{hi} and Ly6C^{lo} cells. Nonmyeloid CD11b^{-} cells harvested during the inflammatory phase of cardiac repair exhibited marked upregulation of chemokines and cytokines; their inflammatory activation was IL-1R1 dependent. Moreover, IL-1β attenuated TGF-β–induced contractile activity of fibroblasts populating collagen pads, attenuated α-smooth muscle actin expression, and stimulated matrix metalloproteinase synthesis in an IL-1R1–dependent manner. The effects of IL-1 on TGF-β responses in cardiac fibroblasts were not due to direct effects on Smad activation, but were associated with endoglin suppression and accentuated expression of bone morphogenetic protein and activin membrane-bound inhibitor, a negative regulator of TGF-β signaling. IL-1 may orchestrate fibroblast responses in the infarct; early stimulation of fibroblast IL-1R1 signaling during the inflammatory phase may prevent premature activation of a matrix-synthetic contractile phenotype until the wound is cleared, and the infarct microenvironment can support mesenchymal cell growth. ***The Journal of Immunology*****, 2013, 191: 4838–4848.**

As the prototypical proinflammatory cytokine, IL-1 drives local and systemic inflammation after injury and is critically involved in the pathobiology of immune and inflammatory conditions (1, 2). A growing body of evidence suggests an important role for IL-1 in the pathogenesis of cardiovascular disease (3). IL-1 is markedly upregulated in atheromatous lesions and may mediate inflammatory changes in diet-induced atherosclerosis (4), accelerating atherosclerotic disease and promoting plaque instability. A double-blind clinical trial examining the effects of IL-1β inhibition on the incidence of new cardiovascular events in diabetic patients with high cardiovascular risk is currently in progress and will test the hypothesis that IL-1β is critically involved in progression and complications of atherosclerotic disease in human patients (5). IL-1β expression is also markedly increased in myocardial infarcts (6) and drives the local inflammatory reaction (7); however, understanding its role in cardiac repair, remodeling, and postinfarction dysfunction is hampered by the cell biological complexity of infarctive injury.

Myocardial inflammation after infarction has both injurious and beneficial aspects. Inflammatory cytokines in the infarcted heart may stimulate cardiomyocyte apoptosis (8, 9), exert negative inotropic actions accentuating systolic dysfunction (10), and induce expression of matrix-degrading proteases promoting dilative cardiac remodeling (11). However, inflammatory cytokines and chemokines also transduce key reparative signals. In addition to their role in clearance of the infarct from dead cells and matrix debris, inflammatory mediators released in the infarcted heart also stimulate expression of fibrogenic and angiogenic growth factors, thus setting the stage for scar formation. Moreover, proinflammatory cytokines, such as TNF-α and IL-1, may activate cytoprotective pathways reducing ischemic cardiomyocyte injury (12, 13); these protective actions may be, at least in part, responsible for the detrimental effects of TNF blockade in patients with heart failure (14). Considering the intense interest in anti–IL-1 strategies for treatment of patients with myocardial infarction and heart failure (15), there is an urgent need to dissect the cell-specific actions of the cytokine in the healing infarct to design optimal therapeutic approaches.

We hypothesized that IL-1–mediated actions on the infarcted myocardium may be mediated through phenotypic modulation of mononuclear cells and cardiac fibroblasts. Using a mouse model of reperfused myocardial infarction, we demonstrate sequential infiltration of the infarcted heart with cells expressing IL-1R1, the only signaling receptor for IL-1, followed by accumulation of cells expressing the decoy receptor IL-1R2. Our experiments identify infarct leukocytes and cardiac fibroblasts as major cellular

*Wilf Family Cardiovascular Research Institute, Division of Cardiology, Department of Medicine, Albert Einstein College of Medicine, Bronx, NY 10461; and †Department of Microbiology and Immunology, Albert Einstein College of Medicine, Bronx, NY 10461

Received for publication March 18, 2013. Accepted for publication August 26, 2013.

This work was supported by National Institutes of Health Grants R01 HL-85440 and R01 HL76246.

Address correspondence and reprint requests to Dr. Nikolaos G. Frangogiannis, Wilf Family Cardiovascular Research Institute, Albert Einstein College of Medicine, 1300 Morris Park Avenue, Forchheimer G46B, Bronx, NY 10461. E-mail address: nikolaos.frangogiannis@einstein.yu.edu

Abbreviations used in this article: ALK, activin receptor–like kinase; BAMBI, bone morphogenetic protein and activin membrane-bound inhibitor; MMP, matrix metalloproteinase; qPCR, quantitative PCR; α-SMA, α-smooth muscle actin; WT, wild-type.

www.jimmunol.org/cgi/doi/10.4049/jimmunol.1300725

targets of IL-1. IL-1R1 signaling is essential for recruitment of both proinflammatory Ly6C^{hi} and reparative Ly6C^{lo} monocytes in the infarct. In contrast, in cardiac fibroblasts, IL-1R1 signaling induces inflammatory activation, stimulates synthesis of matrix-degrading proteins, and attenuates TGF-β–induced myofibroblast transdifferentiation. The effects of IL-1β may involve downregulation of the signaling endoglin receptors and upregulation of the TGF-β pseudoreceptor bone morphogenetic protein and activin membrane-bound inhibitor (BAMBI). During the inflammatory phase of infarct healing, activation of the IL-1 response may prevent premature myofibroblast differentiation, orchestrating the reparative process.

Materials and Methods

Animals

C57BL/6 and IL-1R1$^{-/-}$ (16) mice in a C57BL/6 background were purchased from Jackson Laboratories (Bar Harbor, ME). All protocols were approved by the committee on animal research care at Albert Einstein College of Medicine.

Murine model of reperfused myocardial infarction

Female and male mice (2–3 mo of age) were anesthetized by isoflurane inhalation (isoflurane 2–3% v/v). Myocardial infarction was induced using a closed-chest mouse model of reperfused myocardial infarction, as previously described (6). All animals underwent 1-h coronary occlusion; after 24 h or 7 d of reperfusion, the chest was opened and the heart was immediately excised and processed for either flow cytometric experiments, fibroblast culture experiments, or harvesting of fibroblasts and CD11b^{+} myeloid cells. Sham animals were prepared identically without undergoing coronary occlusion/reperfusion. Mice used to harvest CD11b^{+} cells and fibroblasts for RNA extraction underwent 24 h and 7 d of reperfusion (wild-type [WT], $n = 7$; knockout [KO], $n = 8$ per group). WT mice used for flow cytometric analysis underwent reperfusion at 24 h ($n = 7$) and day 7 ($n = 7$) in addition to uninjured controls ($n = 10$). Flow cytometric studies for the quantitative assessment of the cellular infiltrate at day 7 in WT and IL-1R1 null reperfused infracted hearts included ($n = 5$) in each group.

RNA extraction and quantitative PCR

Total RNA isolated from stimulated cardiac fibroblasts and from CD11b^{+} myeloid and CD11b^{-} nonmyeloid cells was reverse transcribed to cDNA using iScript cDNA synthesis kit (Bio-Rad) following the manufacturer's guidelines. Quantitative PCR (qPCR) was performed using the SYBR green (Bio-Rad) method on the iQ5 Real-Time PCR Detection System (Bio-Rad) for 40 cycles at an annealing temperature (TΔOpt °C) specific for a primer pair as generated by Premier Biosoft. Primers were synthesized using Beacon designer from Premier Biosoft (Version 8.02; Palo Alto, CA). Each sample was run in duplicate. The threshold cycle method using GAPDH or 18S as indicated as the reference gene was used for relative quantification of expression of various genes studied in this study. The following sets of primers were used in the study: IL-1R1 (forward) 5′-CAGGATTCATCAGCAGAA-3′, (reverse) 5′-GAGGCAGTAAGTTGAGTT-3′; IL-1R2 (forward) 5′-GGCTATTACAGATGTGTTATGAC-3′, (reverse) 5′-GTTCCGTGGTTGTTCCTT-3′; Matrix metalloproteinase (MMP)-3 (forward) 5′-GGAAATCAGTTCTGGGCTATACGA-3′, (reverse) 5′-TAGAAATGGCAGCATCGATCTTC-3′; MMP-8 (forward) 5′-GAAGGCAGGAGAGGTTGT-3′, (reverse) 5′-TGGAGGAAGATCAGTAATGGAA-3′; Collagen 1 (forward) 5′-AAGAAGACATCCCTGAAG-3′, (reverse) 5′-ATACAGATCAAGCATACCT-3′; Collagen 3 (forward) 5′-TTGCGATGACATAATCTG-3′, (reverse) 5′-GCACAACATTCTCCAAAT-3′; α-smooth muscle actin (α-SMA) (forward) 5′-GAGTAATGGTTGGAATGG-3′, (reverse) 5′-TGTTCTATCGGATACTTCA-3′; MCP-1 (forward) 5′-AAGTTGACCCGTAAATCT-3′, (reverse) 5′-CTAGTTCACTGTCACACT-3′; IL-10 (forward) 5′-TTGCTATGGTGTCCTTTC-3′, (reverse) 5′-ATCTCCCTGGTTTCTCTT-3′; IL-6 (forward) 5′-GACCATCCAATTCATCTT-3′, (reverse) 5′-CATTCATATTGTCAGTTCTT-3′; IL-1β (forward) 5′-CAAAGAAGAAGATGGAAA-3′, (reverse) 5′-ATGGTGAAGTCAATTATG-3′; GAPDH (forward) 5′-AACGACCCCTTCATTGACCT-3′, (reverse) 5′-CACCAGTAGACTCCACGACA-3′; 18S (forward) 5′-GGCTCATTAAATCAGTTATG-3′, (reverse) 5′-GCTCTAGAATTACCACAG-3′; Activin receptor–like kinase 5 (ALK5) (forward) 5′-ACGAATGACATACTACCTA-3′, (reverse) 5′-CCTGATTATAGCACAAGAG-3′; BAMBI (forward) 5′-GTCTGAACTATAAATGGAACC-3′, (reverse) 5′-TCTCCAAGATGACTAAGC-3′; TNF-α (forward) 5′-GTCTGTATCCTTCTAACTTA-3′, (reverse) 5′-TCTTGTGTTTCTGAGTAG-3′; Endoglin-L (forward) 5′-CGTAATGATGGAACTGAG-3′, (reverse) 5′-ATGAACCAGGAGACATAT-3′, Endoglin-S (forward) 5′-CGTAATGATGGAACTGAG-3′, (reverse) 5′-ATGAACCAGGAGACATAT-3′, periostin (forward) 5′-TGCCAACAGTTACTATGA-3′, (reverse) 5′-CAGCATTCATATAGCACAG-3′.

Flow cytometry in cells harvested from control and infarcted hearts

Single-cell suspensions were obtained from infarcted WT and IL-1R1 null hearts as previously described (17). Cells harvested from the infarcted heart were counted and reconstituted in staining buffer (BD Biosciences) to a concentration of 1×10^6 cells/ml. Subsequently, cells were incubated with LIVE/DEAD Fixable Dead Cell Stain single-color dyes (Invitrogen) for 30 min at room temperature to evaluate the viability. After one rinse with washing buffer, cells were incubated with anti-FcγIII/II (clone 2.4G2) Ab (BD Pharmingen) for 15 min and labeled at 4°C for 30 min simultaneously with the following rat anti-mouse Abs purchased from Biolegend: PerCP-labeled anti-CD45, FITC-labeled anti-CD11b, PE-Cy7–labeled anti-F4/80, allophycocyanin-labeled anti–IL-1R1 and Pacific blue–labeled anti-CD19. Allophycocyanin-Cy7–labeled anti-Ly6C was from BD Pharmingen. For intracellular staining, cells were fixed and permeabilized for 20 min at 4°C with fixation/permeabilization kit (eBioscience). Subsequently, cells were incubated with PE-labeled anti–IL-1β (BD Pharmingen). Finally, cells were washed twice, resuspended in staining buffer, and immediately analyzed with a Becton Dickinson LSRII flow cytometer (BD Biosciences). Cell analysis using flow cytometry included analysis of only singlet cells; all doublets were excluded from the analysis by monitoring the side scatter/forward scatter pulse width channel.

Monocytes/macrophages were defined as Live/dead^{low}CD19−CD45^{high} CD11b^{high} cells. Within this population, subsets were identified as either F4/80^{+} or F4/80^{-}. Further, each F4/80 subgroup was identified as either Ly-6C^{hi} or Ly-6C^{lo}. The absolute number of cells in each subset was calculated by multiplying cell number by percent of cells in the subset, which was calibrated by heart weight and expressed as cells per milligram. Data analysis was performed using FlowJo (Tree Star).

Isolation of CD11b^{+} myeloid cells and CD11b^{-} nonmyeloid cells from infarcted hearts

CD11b^{+} myeloid cells and CD11b^{-} fibroblasts were isolated from control and infarcted hearts for RNA extraction. In brief, infarct tissue (1-h ischemia followed by 24 h or 7 d of reperfusion) or healthy hearts were minced and placed into a mixture of 0.25 mg/ml Liberase Blendzyme 3 (Roche Applied Science), 20 U/ml DNase I (Sigma Aldrich), 10 mmol/l HEPES (Invitrogen), 0.1% sodium azide in HBSS with Ca^{2+} and Mg^{2+} (Invitrogen), and shaken at 37°C for 40 min. Subsequently, cells were passed through 40-μm nylon mesh and centrifuged (10 min, $200 \times g$, 4°C). Finally, cells were reconstituted with staining buffer (d-PBS without Ca^{2+} and Mg^{2+}, 2% FBS, 0.1% sodium azide), and total cell numbers were determined with trypan blue (Mediatech). The resulting single-cell suspensions were washed with HBSS supplemented with 0.2% (w/v) BSA and 1% (w/v) FCS, and centrifuged. Single cells were resuspended in a special MACS buffer containing PBS, pH 7.2, 0.5% BSA, and 2 mM EDTA, incubated with CD11b^{+} microbeads (Miltenyi Biotec) 10 μl/10^7 cells at 4°C for 15 min, then washed once and centrifuged. Resuspended cells went through a MACS Column (Miltenyi Biotec) set in a MACS Separator (Miltenyi Biotec). Unlabeled cells that passed through were collected and washed once with PBS as the CD11b^{-} fraction. These CD11b^{-} cells were harvested for further experiments. The magnetically labeled CD11b^{+} cells were retained on the column. Approximately 2 ml MACS buffer was applied onto the column. Cells were flushed out by firmly pushing the plunger and collected into a tube.

Protein extraction and Western blotting

Fibroblasts harvested from WT and IL-1R1 null hearts underwent stimulation with IL-1β (10 ng/ml) or LPS (25 ng/ml) for 15–60 min, to assess activation of p-Smad2/Smad2 and pErk1/2. At the end of the experiment, cell lysates were used for protein extraction. Western blotting was performed as previously described using Abs to p-Smad2, Smad2/3 (Cell Signaling), and GAPDH. The ratio of p-Smad2/Smad2 expression was assessed.

Assessment of contraction of collagen pads populated with cardiac fibroblasts

To assess the contractile properties of cardiac myofibroblasts, we used collagen pads populated with cardiac fibroblasts as previously described (18). After polymerization, fibroblast-populated collagen pads were incu-

bated in triplicates (WT; $n = 9$) or duplicates (IL-1R1$^{-/-}$; $n = 6$) of three individual pads in each six-well culture plate (BD Falcon, San Jose, CA) with the following conditions: 0% FCS DMEM (1×), 15 ng/ml IL-1β, and TGF-β (10 ng/ml) in the presence or absence of 15 ng/ml IL-1β. After 24 h, the pictures of the plates were taken in flatbed scanner, and the area of each pad was measured using Image Pro software. To study expression of MMPs and TGF-βRs in fibroblasts populating the collagen pads, we performed RNA extraction at the end of the experiment.

Assessment of myofibroblast transdifferentiation and matrix protein synthesis by isolated cardiac fibroblasts

Cardiac fibroblasts from WT and IL-1R1$^{-/-}$ hearts were isolated by enzymatic digestion with a collagenase buffer as previously described (18, 19). Cells at passage 3 were seeded in chambers of Culture Slides (BD Falcon) and allowed to attach overnight. Cells were serum-starved for 24 h and subsequently stimulated with 25 ng/ml TGF-β1 (R&D Systems) in the presence or absence of IL-1β (15 ng/ml) for 24 or 72 h. Cells were harvested and total RNA extracted using TRIzol (Invitrogen). Additional cells were fixed for 10 min in a 3.7% solution of paraformaldehyde (Sigma), then washed twice with PBS and stained for α-SMA. qPCR was performed to measure expression of collagen I, periostin, and α-SMA. Immunofluorescence was performed after permeabilization with 0.1% Triton-X (Sigma) in PBS. Subsequently, slides were stained with FITC-labeled anti–α-SMA Ab (Sigma). Finally, to visualize the polymerized actin cytoskeleton, we incubated slides in 0.5 μM solution of Alexa Fluor 594–conjugated phalloidin (Molecular Probes) in PBS for 20 min. Nuclei were stained with DAPI (Invitrogen).

Statistical analysis

Data are expressed as mean ± SEM. Statistical analysis was performed using GraphPad version 5 (GraphPad Software, La Jolla, CA) using unpaired, two-tailed Student t test using Welch's correction for unequal variances and one-way ANOVA with Tukey's multiple-comparison test. Results were considered statistically significant at $p < 0.05$.

Results

Sequential infiltration of the infarcted myocardium with monocyte subpopulations

To study the time course of infiltration of the infarct with monocyte subpopulations, we performed flow cytometric analysis of cells harvested from the infarcted mouse myocardium. Reperfused myocardial infarction had intense infiltration with CD45$^+$ hematopoietic cells (Fig. 1A) that peaked after 24 h of reperfusion (Fig. 1A, 1B). The number of CD45$^+$/CD11b$^+$ myeloid cells (Fig. 1C) and of CD45$^+$/F4/80$^+$ macrophages (Fig. 1D) also peaked after 24 h of reperfusion showing a 20-fold increase in comparison with control myocardium. Ly6C identifies a "proinflammatory" monocyte phenotype (Ly6C^{hi}) that infiltrates the inflamed tissue during the early stages after injury; in contrast, Ly6C^{lo} cells have reduced inflammatory activity and exhibit reparative properties (20). In the reperfused mouse infarct, abundant CD11b$^+$/Ly6C^{hi} proinflammatory monocytes were recruited in the infarcted myocardium during the peak of the inflammatory phase (24 h of reperfusion; Fig. 1A–E). Subsequently, the number of Ly6C^{hi} cells decreased significantly after 3–7 d of reperfusion, reflecting resolution of the inflammatory infiltrate. In contrast, the number of CD11b$^+$/Ly6C^{lo} cells increased markedly after 7 d of reperfusion (Fig. 1F), reflecting late infiltration of the infarct with reparative monocytes.

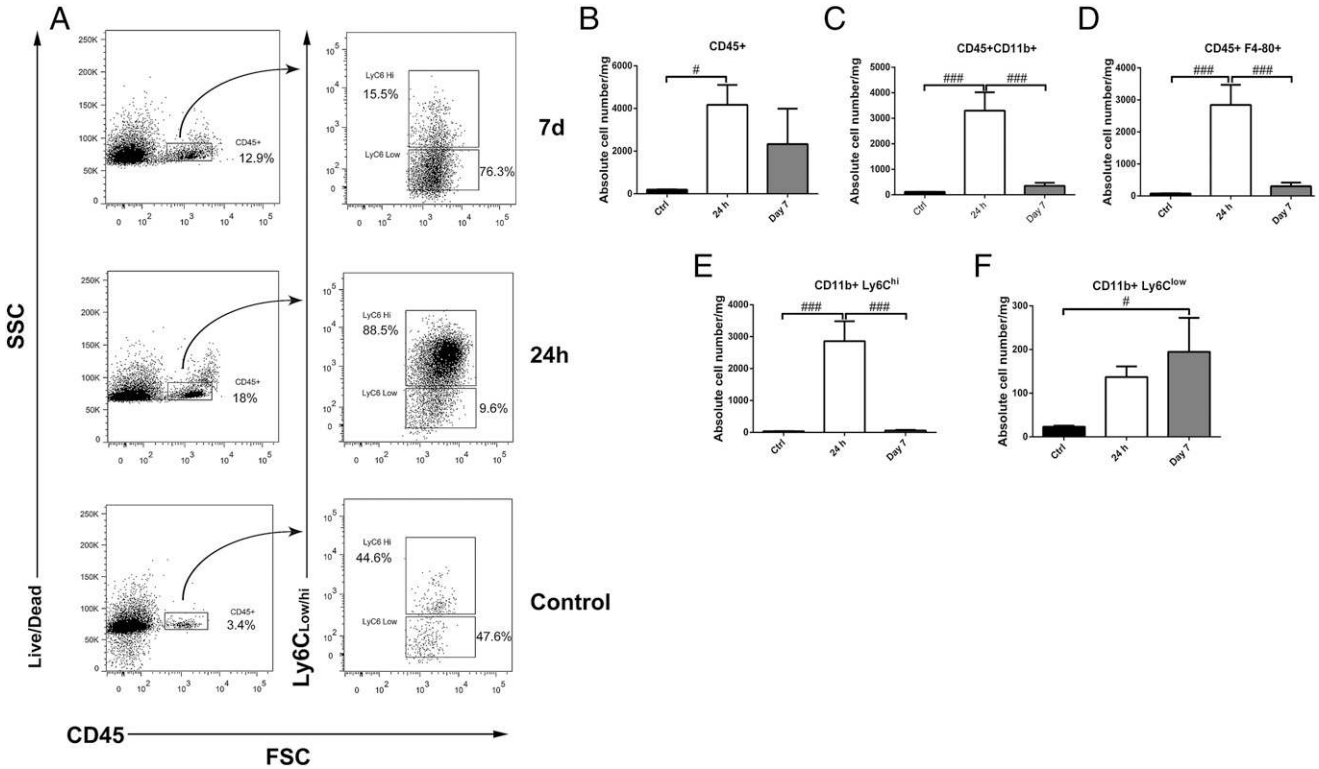

FIGURE 1. Sequential infiltration of the infarcted mouse heart with proinflammatory and reparative monocytes subpopulations. Noncardiomyocytes were harvested from control and infarcted mouse hearts after 24 h of reperfusion (inflammatory phase) and after 7 d of reperfusion (proliferative phase). Total cells were separated as Live/Dead, and gated CD45$^+$ cells were quantified (as shown in the forward scatter/side scatter dot plot). Flow cytometric analysis (**A**) showed marked infiltration of the infarcted heart with CD45$^+$ hematopoietic cells that peaked after 24 h of reperfusion (**B**). The number of CD45$^+$/CD11b$^+$ myeloid cells (**C**) and CD45$^+$/F4/80$^+$ macrophages (**D**) was markedly increased after 24 h of reperfusion and was significantly reduced after 7 d, reflecting clearance of the inflammatory infiltrate. Flow cytometry for Ly6C was used to identify proinflammatory Ly6C^{hi} and reparative Ly6C^{lo} monocytes subpopulations (**E**). The number of proinflammatory CD11b$^+$/Ly6C^{hi} monocytes markedly increased after 24 h of reperfusion, then decreased during the proliferative phase after 7 d of reperfusion (**F**). In contrast, the number of reparative CD11b$^+$/Ly6C^{lo} cells was increased after 7 d of reperfusion. $^{\#}p < 0.05$, $^{\#\#\#}p < 0.001$.

IL-1R expression profile in cells infiltrating the infarcted myocardium

Changes in relative expression of the signaling, IL-1R1, and the decoy receptor, IL-1R2, may determine responsiveness to the cytokine. Thus, transition from the inflammatory to the resolution phase of the postinfarction reparative response may be characterized with dynamic alterations in IL-1R1 and IL-1R2 expression by inflammatory leukocytes. We used flow cytometry to study the IL-1R expression profile in cells harvested from reperfused infarcted hearts (Fig. 2A). The number of IL-1R1$^+$ cells in the infarcted myocardium peaked after 24 h of reperfusion. In comparison with control hearts, the infarcted myocardium showed marked, but transient, increases in the number of IL-1R1–expressing CD45$^+$ hematopoietic cells (130-fold), IL-1R1$^+$ CD11b$^+$ myeloid cells (42-fold), and IL-1R1$^+$ F4/80$^+$ macrophages (158-fold; Fig. 2B–E) after 24 h of reperfusion. After 7 d of reperfusion, the number of IL-1R1$^+$ hematopoietic cells decreased significantly, suggesting either clearance of IL-1R1–expressing leukocytes or suppressed expression of the signaling receptor (Fig. 2B–E).

In contrast, much like Ly6C^{lo} monocytes, IL-1R2$^+$/CD45$^+$ hematopoietic cells appeared late in the infarcted myocardium (Fig. 2A, 2F–I). After 7 d of reperfusion, infarcted hearts exhibited a 36-fold increase in the number of IL-1R2$^+$/CD11b$^+$ myeloid cells and a 45-fold increase in the number of IL-1R2–expressing F4/80 macrophages (Fig. 2F–I).

IL-1R expression profile in Ly6C^{hi} and Ly6C^{lo} cells

Because the time course of infiltration with proinflammatory Ly6C^{hi} monocytes resembled the time course of recruitment of IL-1R1$^+$ cells, we asked whether the proinflammatory phenotype of Ly6C^{hi} cells may be caused by increased expression of IL-1R1, thus reflecting increased responsiveness to the inflammatory actions of IL-1. Ly6C^{lo} cells, in contrast, may exhibit attenuated proinflammatory signaling because of expression of the IL-1R2 decoy receptor. Using flow cytometry, we examined the IL-1R expression profile in Ly6C^{hi} and Ly6C^{lo} cells harvested from the infarcted mouse heart. IL-1R1 and IL-1R2$^+$ cells were found in both Ly6C^{hi} and Ly6C^{lo} subpopulations. The number of IL-1R1$^+$/Ly6C^{hi} cells peaked during the early inflammatory phase of infarct healing (after 24 h of reperfusion) and was significantly reduced during the proliferative phase (after 7 d of reperfusion; Fig. 3A, Table I). In contrast, the number of IL-1R1$^+$/Ly6C^{lo} cells was very low (Fig. 3B, Table I). Cells expressing the decoy receptor IL-1R2 were more abundant during the reparative phase (after 7 d of reperfusion; Fig. 3C, 3D; Table I). At all time points examined, the majority of IL-1R1$^+$ hematopoietic cells were Ly6C^{hi} (control: 54.1 + 12%, 24 h: 58.7 + 6.7%, 7 d: 60.7 + 7.9%), whereas a significantly lower percentage of IL-1R1$^+$ cells was identified as Ly6C^{lo} cells (control: 30.1 + 7.1%, 24 h: 1.7 + 0.5%, 7 d: 32 + 10%). Relative expression of IL-1Rs by Ly6C^{lo} and Ly6C^{hi} subsets was dependent on the stage of healing as evidenced by dynamic changes in the ratio of IL-1R2$^+$ to IL-1R1$^+$ cells within the Ly6C^{hi} and Ly6C^{lo} subpopulations (Table I). During the inflammatory phase of infarct healing, IL-1R1$^+$/Ly6C^{hi} cells outnumbered IL-1R2$^+$/Ly6C^{hi} cells by 15:1, whereas after 7 d of reperfusion, comparable numbers of IL-1R1$^+$ and IL-1R2$^+$ Ly6C^{hi} cells were identified. In the Ly6C^{lo} subpopulation, the ratio of IL-1R1$^+$/IL-1R2$^+$ cells was also significantly lower after 7 d of reperfusion, reflecting

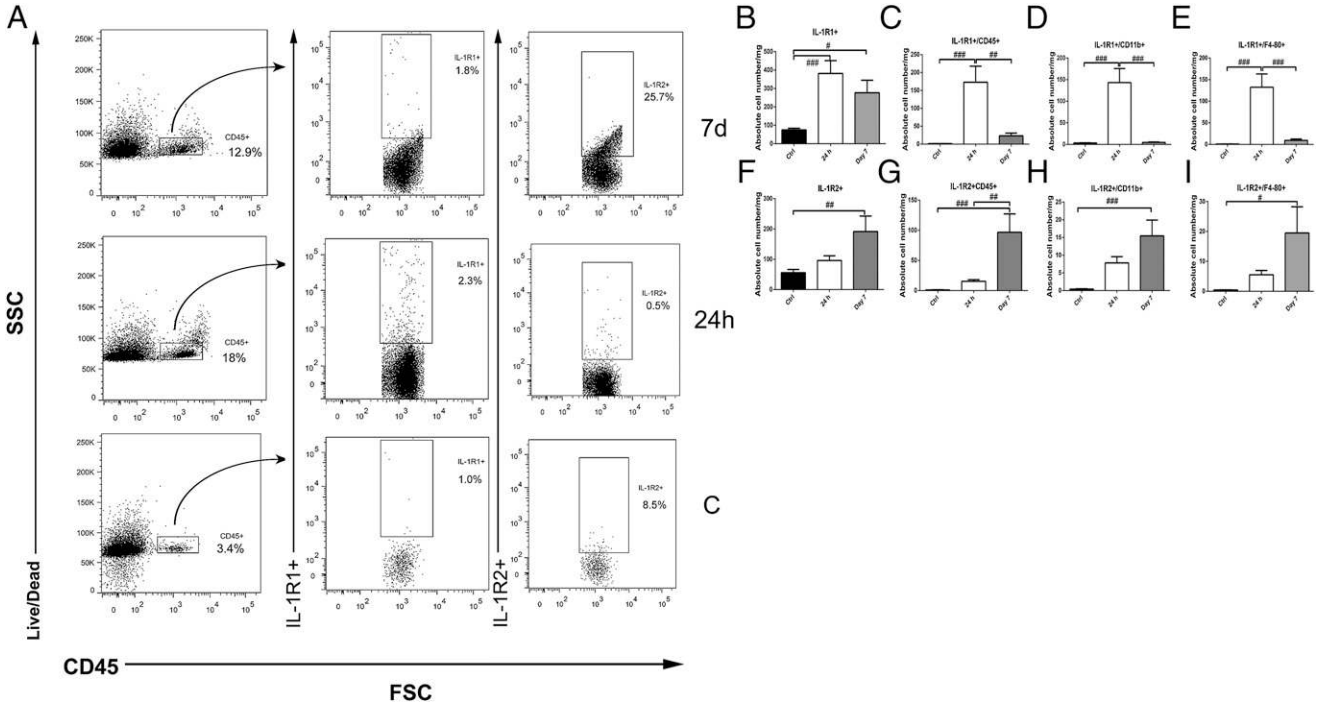

FIGURE 2. Sequential infiltration of the infarcted myocardium with IL-1R1$^+$ and IL-1R2$^+$ cells. Fluorescently labeled CD45$^+$ cells were gated for IL-1R1$^+$, the only signaling receptor for IL-1, and IL-1R2$^+$ (decoy receptor), which were spectrally resolved and quantified (**A**). (**B**) A significant increase in IL-1R1$^+$ cells was noted during the inflammatory phase of cardiac repair (24 h of reperfusion). Marked, but transient, increase in the number of IL-1R1$^+$/CD45$^+$ hematopoietic cells (**C**), IL-1R1$^+$/CD11b$^+$ myeloid cells (**D**), and IL-1R1$^+$/F4/80$^+$ macrophages (**E**) was noted after 24 h of reperfusion. In contrast, late infiltration of the infarct with IL-1R2$^+$ cells was noted. The number of IL-1R2$^+$ cells (**F**), IL-1R2$^+$/CD45$^+$ hematopoietic cells (**G**), IL-1R2$^+$/CD11b$^+$ myeloid cells (**H**), and IL-1R2$^+$/F4/80$^+$ macrophages (**I**) increased significantly after 7 d of reperfusion. Early recruitment of IL-1–responsive IL-1R1$^+$ cells may play an important role in activation of the inflammatory leukocyte response. In contrast, late infiltration of cells expressing the decoy receptor may serve as a mechanism for termination of IL-1 signaling. C, Control; 24h, 1h ischemia/24h reperfusion; 7d, 1h ischemia/7 days reperfusion.

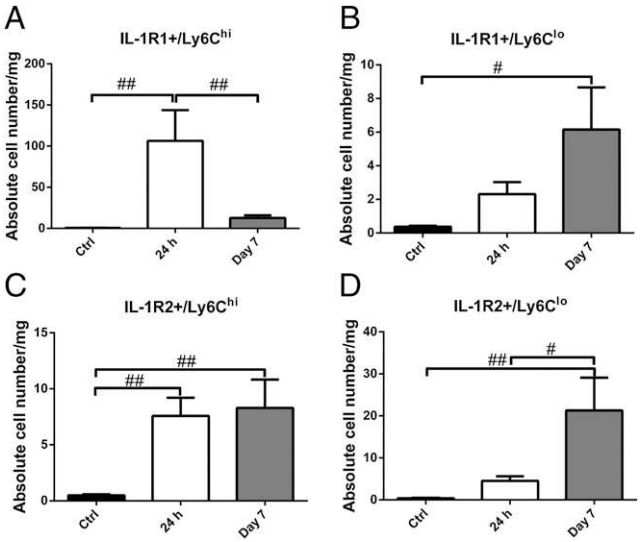

FIGURE 3. Relation between IL-1R expression and Ly6C levels in leukocytes infiltrating the infarcted heart. Flow cytometry of cells harvested from infarcted and controls hearts demonstrated that the number of IL-1R1$^+$/Ly6C^{hi} cells markedly increased after 24 h of reperfusion (**A**); in contrast, IL-1R1$^+$/Ly6C^{lo} cells were much less abundant (**B**) and their number increased after 7 d of reperfusion. Small numbers of IL-1R2$^+$/Ly6C^{hi} cells were found in the infarct after 24 h/7 d of reperfusion (**C**). (**D**) Consistent with their reparative, anti-inflammatory phenotype, IL-1R2$^+$/Ly6C^{lo} infiltrate the myocardium during the proliferative phase (after 7 d of reperfusion). $^{\#}p < 0.05$, $^{\#\#}p < 0.01$.

increased expression of the decoy receptor by Ly6C^{lo} cells in the late phases of infarct healing (Table I).

IL-1R1 signaling mediates inflammatory leukocyte recruitment in the infarcted myocardium

We have previously demonstrated that IL-1R1 null mice exhibit attenuated adverse remodeling after myocardial infarction, associated with reduced myocardial expression of inflammatory cytokines and chemokines (7). We hypothesized that attenuated inflammatory activity in IL-1R1 KO animals may be caused by decreased recruitment of proinflammatory leukocytes. Accordingly, we quantitatively assessed the cellular infiltrate in WT and IL-1R1 null hearts using flow cytometry. When compared with WT animals, IL-1R1 null mice exhibited a marked reduction in the total number of infarct cells after 7 d of reperfusion (Table II). Decreased cellular infiltration in the infarcted myocardium was due to reduced recruitment of CD45$^+$ hematopoietic cells (Table II). In contrast, the number of CD45$^-$ cells was comparable between WT and IL-1R1 KO infarcted hearts (Table II). IL-1R1 loss was associated with markedly reduced infiltration of the infarct with CD11b$^+$, Ly6C^{hi}, and Ly6C^{lo} cells, suggesting that IL-1 signaling plays an essential role in mediating the postinfarction inflammatory response (Table II).

Disruption of IL-1 signaling in IL-1R1 null mice is associated with attenuated inflammatory activity in CD11b$^-$ myeloid cells

In addition to its effects on monocyte nonrecruitment in the infarcted myocardium, IL-1R1 signaling may increase the level of proinflammatory activation of fibroblasts and leukocytes in the infarcted heart. To dissect the cellular targets of IL-1–mediated proinflammatory actions, we harvested CD11b$^+$ leukocytes and CD11b$^-$ nonmyeloid cells from control and infarcted WT and IL-1R1 null hearts, and we compared expression of proinflammatory cytokines. In comparison with cells harvested from normal hearts, CD11b$^+$ myeloid cells and CD11b$^-$ nonmyeloid cells harvested from infarcts after 24 h of reperfusion showed markedly increased IL-1β and MCP-1 mRNA expression (Fig. 4A, 4B, 4D, 4E).

CD11b$^-$ cells isolated from IL-1R1 null infarcts after 24 h of reperfusion had markedly lower IL-1β (Fig. 4A) and MCP-1 (Fig. 4B) expression than WT infarct CD11b$^-$ cells harvested at the same postreperfusion time point. In contrast, in CD11b$^+$ leukocytes, cytokine and chemokine expression levels were not affected by IL-1R1 loss (Fig. 4D, 4E). IL-6 mRNA expression showed a distinct time course of expression in CD11b$^+$ leukocytes and in CD11b$^-$ nonmyeloid cells: CD11b$^-$ cells exhibited early upregulation after 24 h of reperfusion (Fig. 4C), whereas CD11b$^+$ leukocytes had a late increase after 7 d (Fig. 4C–F). IL-1R1 disruption did not significantly affect IL-6 expression by infarct leukocytes and nonmyeloid cells (Fig. 4C, 4F).

IL-1R expression profile in infarct fibroblasts

Because loss of IL-1 signaling selectively attenuated inflammatory activation of nonmyeloid cells, we studied the IL-1R expression profile in CD11b$^-$ cells isolated from infarcted hearts. IL-1R1 mRNA expression was significantly increased in CD11b$^-$ cells harvested after 24 h of reperfusion when compared with corresponding nonmyeloid cells from control hearts (Fig. 5A). In

Table I. Flow cytometric analysis of inflammatory cells shows sequential infiltration of the infarcted heart with IL-1R1$^+$ and IL-1R2$^+$ cells

Absolute Cell Number (Cells/mg)	Control	24 h	Day 7
CD45$^+$	198.62 ± 16	4,170.79 ± 931*	2,334.33 ± 1660
CD45$^-$	5,895.73 ± 337.1	10,809.08 ± 1790**	6,329.00 ± 955.6
CD45$^+$/CD11b$^+$	119.77 ± 10.79	3,301.94 ± 715.9***	353.52 ± 119
CD45$^+$/Ly6C^{hi}	60.52 ± 5.19	3,611.86 ± 811.2**	470.36 ± 352.1
CD45$^+$/Ly6C^{lo}	38.09 ± 3.58	173.12 ± 31.17	886.52 ± 517.8
CD45$^+$/CD11b$^+$/Ly6C^{hi}	36.83 ± 3.83	2,859.90 ± 623.5***	60.77 ± 16.06
CD45$^+$/CD11b$^+$/Ly6C^{lo}	23.14 ± 2.50	136.99 ± 24.31	194.54 ± 78.03*
CD45$^+$/F4/80$^+$	78.85 ± 7.63	2,846.47 ± 626.3***	306.05 ± 112.5
IL-1R1$^+$	75.20 ± 8.95	381.77 ± 69.78***	276.90 ± 67.73
IL-1R2$^+$	55.75 ± 10.63	96.08 ± 15.66	191.72 ± 50.84*
IL-1R1$^+$/Ly6C^{hi}	0.66 ± 0.14	106.35 ± 37.36**	12.75 ± 3.11
IL-1R1$^+$/Ly6C^{lo}	0.37 ± 0.06	2.31 ± 0.71	6.15 ± 2.50*
IL-1R2$^+$/Ly6C^{hi}	0.49 ± 0.07	7.58 ± 1.62 **	8.29 ± 2.52
IL-1R2$^+$/Ly6C^{lo}	0.39 ± 0.07	4.52 ± 1.09	21.26 ± 7.81*
IL-1R1$^+$/Ly6C^{hi}: IL-1R2$^+$/Ly6C^{hi}	1.69 ± 0.5	15.22 ± 5.49	2.06 ± 0.55
IL-1R1$^+$/Ly6C^{lo}: IL-1R2$^+$Ly6C^{lo}	1.28 ± 0.1	0.61 ± 0.15	0.31 ± 0.05

$^*p < 0.05$, $^{**}p < 0.01$, $^{***}p < 0.001$ versus corresponding control.

Table II. Comparison of the inflammatory infiltrate in the infarcted heart (1 h ischemia/7 d reperfusion) between WT and IL-1R1$^{-/-}$ mice

Absolute Cell Number (Cells/mg)	WT (Day 7)	IL-1R1$^{-/-}$ (Day 7)
Total cell number	18091.00 ± 2833*	10166.09 ± 1877
CD45$^+$	5211.77 ± 1170**	1624.54 ± 200.2
CD45$^-$	9123 ± 1219	7558 ± 1515
CD45$^+$/CD11b$^+$	4554.11 ± 1070**	1196.94 ± 160.5
CD45$^+$/Ly6C^{hi}	3271.31 ± 881.0*	647.16 ± 88.99
CD45$^+$/Ly6C^{lo}	1247.64 ± 383.9	453.68 ± 120.2

*$p < 0.05$, **$p < 0.01$ versus IL-1R1$^{-/-}$.

contrast, IL-1R2 mRNA expression was not detected in nonmyeloid cells harvested from the infarcted heart (data not shown). Because fibroblasts represent the majority of interstitial nonmyeloid cells in control and infarcted hearts, we examined whether inflammatory cytokines regulate IL-1R1 mRNA expression in isolated cardiac fibroblasts. In cardiac fibroblasts harvested from normal WT mice, IL-1β significantly induced IL-1R1 mRNA synthesis after 4 h of stimulation (Fig. 5B). In contrast, IL-10 and TGF-β stimulation did not modulate fibroblast-derived IL-1R1 mRNA synthesis (Fig. 5B).

IL-1β abrogates TGF-β–induced contraction of fibroblast-populated collagen pads in an IL-1R1–dependent manner

Although in the early stages after cardiac injury, fibroblasts may function as proinflammatory cells, the most dramatic alterations in their phenotype occur during the proliferative phase, when infarct fibroblasts undergo myofibroblast transdifferentiation. Acquisition of the myofibroblast phenotype is associated with increased expression of contractile proteins, such as α-SMA, and induces scar contraction. To study the effects of IL-1 on myofibroblast transdifferentiation, we used a fibroblast-populated collagen pad assay. As previously reported by our laboratory (19), TGF-β, the key mediator in myofibroblast transdifferentiation, induced significant contraction of fibroblast-populated collagen pads (Fig. 6A). IL-1β stimulation abolished TGF-β–induced gel contraction in pads populated with WT cells. The effects of IL-1β were dependent on IL-1R1 signaling; in collagen pads populated with IL-1R1 null cells, IL-1 stimulation did not modulate TGF-β–induced gel contraction (Fig. 6A). Moreover, unstimulated IL-1R1 null fibroblasts induced increased gel contraction when compared with WT cells, suggesting that loss of IL-1 signaling may allow unopposed actions of autocrine or paracrine growth factors (Fig. 6A).

IL-1β attenuates α-SMA expression in stimulated cardiac fibroblasts

Reduced gel contraction upon stimulation with IL-1β likely reflects impaired myofibroblast transdifferentiation. Accordingly, we examined whether IL-1β modulates α-SMA expression in stimulated fibroblasts. Unstimulated cardiac fibroblasts exhibited high expression of α-SMA after 24–72 h of culture (Fig. 6B, 6C); stimulation with IL-1β significantly suppressed α-SMA mRNA synthesis in both control and TGF-β–stimulated cells (Fig. 6B, 6C). The effects of IL-1β were abrogated in IL-1RI KO cells (Fig. 6B, 6C). Immunofluorescent staining of isolated fibroblasts for α-SMA supported the qPCR data showing that IL-1β reduced the incorporation of α-SMA in the cytoskeleton in an IL-1RI–dependent manner (Fig. 6D). IL-1β also suppressed TGF-β–induced expression of the matricellular protein periostin (Fig. 6G, 6H), a key modulator of fibroblast phenotype and function in the infarcted and remodeling myocardium (21, 22). The effects of IL-1β on periostin synthesis were dependent on signaling through the type 1 receptor (Fig. 6H). In contrast, expression of collagen type I mRNA by TGF-β–stimulated fibroblasts was not consistently modulated by IL-1β (Fig. 6E, 6F).

IL-1β does not modulate TGF-β–induced Smad2/3 phosphorylation

Because TGF-β/Smad3 signaling is critically involved in cardiac myofibroblast transdifferentiation, we examined whether IL-1 directly modulates TGF-β–induced Smad2/3 activation. After 60 min of incubation, TGF-β stimulation significantly increased the levels of p-Smad2 in cardiac fibroblasts (*$p < 0.05$); however, coincubation with IL-1β did not alter Smad2 phosphorylation (Fig. 6B, 6C).

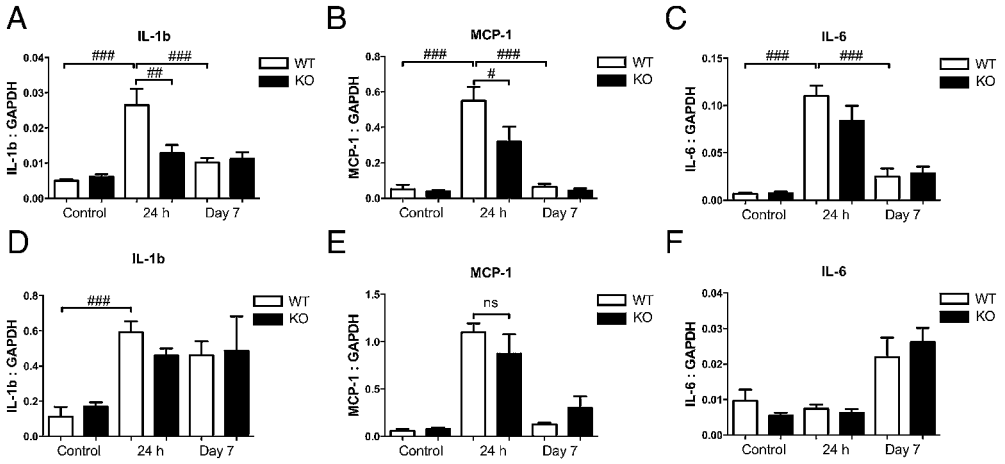

FIGURE 4. IL-1R1 loss is associated with attenuated inflammatory activity in CD11b$^-$ nonmyeloid cells harvested from the infarct but does not affect cytokine and chemokine synthesis by CD11b$^+$ myeloid cells. CD11b$^-$ nonmyeloid cells isolated from myocardial infarcts at the peak of the inflammatory phase (24-h reperfusion) had increased expression of IL-1β (**A**), MCP-1 (**B**), and IL-6 (**C**) when compared with cells isolated from control hearts. In contrast, in CD11b$^-$ cells harvested after 7 d of reperfusion, expression of proinflammatory cytokines and chemokines was comparable with control cells. IL-1R1 loss significantly attenuated IL-1β (A) and MCP-1 (B) expression in inflammatory phase CD11b$^-$ cells but did not affect IL-6 synthesis (C) ($^{\#}p < 0.05$ versus corresponding WT). CD11b$^+$ myeloid cells harvested from the infarcted heart after 24 h of reperfusion had significantly higher expression of IL-1β (**D**) and MCP-1 (**E**), but not IL-6 (**F**), in comparison with CD11b$^+$ cells harvested from control hearts. However, IL-1R1 loss did not affect expression of inflammatory cytokines and chemokines in myeloid cells ($^{\#\#}p < 0.01$, $^{\#\#\#}p < 0.001$).

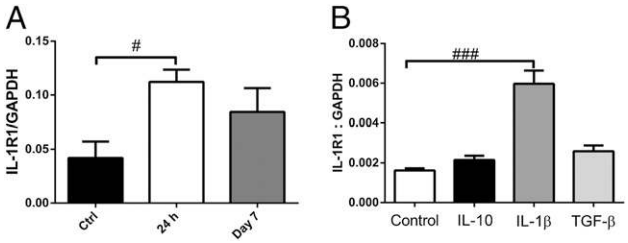

FIGURE 5. IL-1R1 regulation in isolated cardiac fibroblasts. (**A**) $CD11b^-$ cells harvested from mouse infarcts after 24 h of reperfusion had increased expression of IL-1R1 ($^{\#}p < 0.05$). (**B**) IL-1β markedly upregulated IL-1R1 expression in cardiac fibroblasts ($^{\#\#\#}p < 0.001$ versus control); in contrast, TGF-β and IL-10 had no effects.

IL-1β stimulation inhibits endoglin expression in cardiac fibroblasts and enhances TGF-β–induced synthesis of the decoy TGF-βR BAMBI

Next, we asked whether the inhibitory effects of IL-1β on TGF-β–induced fibroblast contractile activity are due to modulation of TGF-βR expression. TGF-β, but not IL-1β, stimulated mRNA expression of the TGF-β type I receptor ALK5; costimulation with IL-1β did not affect TGF-induced ALK5 synthesis (Fig. 7A). IL-1β stimulation suppressed expression of the TGF-β coreceptor endoglin, inhibiting synthesis of both endoglin-L and endoglin-S transcripts, but did not modulate endoglin expression by TGF-β–stimulated cells (Fig. 7B, 7C). The TGF-β decoy receptor BAMBI participates in negative regulation of TGF-β signaling; accordingly, we examined whether IL-1β inhibits TGF-β responses by increasing BAMBI expression in cardiac fibroblasts. Although IL-1β stimulation did not alter BAMBI mRNA expression in cardiac fibroblasts, costimulation with TGF-β and IL-1β significantly upregulated BAMBI mRNA (Fig. 7D). Cardiac fibroblasts harvested from IL-1R1 KO mice had lower baseline expression of ALK5, endoglin-L, and endoglin-S when compared with WT fibroblasts (Fig. 7E–G). The inhibitory effects of IL-1β on endoglins were dependent on IL-1R1 signaling (Fig. 7F, 7G). Moreover, the effects of IL-1β/TGF-β costimulation on BAMBI synthesis were also abrogated in IL-1R1 null cells (Fig. 7H).

IL-1 enhances expression of the collagenases MMP-3 and MMP-8 in cardiac fibroblasts in an IL-1R1–dependent manner

To explore the effects of IL-1 on the matrix-degrading potential of cardiac fibroblasts, we assessed expression of the collagenases MMP-3 and -8 by IL-1–stimulated fibroblasts cultured in collagen pads. After 24 h of stimulation, IL-1β markedly induced MMP-3 and -8 mRNA synthesis; the effects of IL-1 were abrogated in IL-1R1 null fibroblasts.

Discussion

In the infarcted heart, dying cardiomyocytes generate danger signals triggering an intense inflammatory reaction that leads to infiltration of the infarct with leukocytes (20, 23). Although the postinfarction inflammatory response is required to clear the wound from dead cells and matrix debris, and to promote repair of the infarcted tissue, it is also closely intertwined with ventricular remodeling, a constellation of molecular, proteomic, and cellular changes that involve both the infarcted and the noninfarcted myocardium leading to chamber dilation and to the development of systolic dysfunction. We have previously demonstrated that IL-1 signaling plays a central role in myocardial inflammation and dilative remodeling after myocardial infarction (7). In this study, we used mice lacking expression of IL-1R1, the only signaling receptor for IL-1, to explore the cell biological actions of IL-1 in the infarcted and remodeling heart. We report for the first time, to our knowledge, that the effects of IL-1 on the infarcted myocardium are mediated through cell-specific proinflammatory and antifibrotic effects on infarct mononuclear cells and fibroblasts. IL-1R1 loss is associated with a global attenuation of the postinfarction inflammatory response and with impaired recruitment of both proinflammatory and reparative monocytes. Cardiac fibroblasts are also highly responsive to the effects of IL-1. IL-1R1 signaling not only induces proinflammatory activation of cardiac fibroblasts, but also inhibits myofibroblast transdifferentiation and promotes a matrix-degrading phenotype. Our findings demonstrate that IL-1 is an essential mediator in postinfarction cardiac remodeling and orchestrates the reparative response preventing premature activation of myofibroblasts during the inflammatory phase of infarct healing.

Sequential infiltration of the infarcted heart with IL-1R1 and IL-1R2 cells may regulate the postinfarction inflammatory response

In the infarcted heart, sequential recruitment of leukocyte subpopulations with distinct properties may play an important role in regulation of inflammatory and reparative responses. Early recruitment of proinflammatory $Ly6C^{hi}$ monocytes through interactions that involve MCP-1/CCR2 signaling (20, 23) mediates phagocytotic clearance of dead cells and matrix debris from the infarct. These cells may be involved in the pathogenesis of dilative remodeling by producing and activating proteases, thus degrading the extracellular matrix. During the reparative phase of healing, the profile of infarct monocytes changes is that reparative $Ly6C^{lo}$ cells with high expression of the fractalkine receptor CX3CR1 accumulate in the infarct and may mediate angiogenic and profibrotic responses (20). Our findings provide further support for the presence of a biphasic monocytic response in reperfused myocardial infarcts (Table I). Flow cytometric analysis demonstrated that at the peak of the inflammatory phase (after 24 h of reperfusion), the number of proinflammatory $Ly6C^{hi}$ cells increased 60-fold in the infarcted myocardium, whereas the number of reparative $Ly6C^{lo}$ cells was only modestly elevated (4-fold increase versus control myocardium). In contrast, during the proliferative phase (after 7-d reperfusion), the number of $Ly6C^{hi}$ cells was markedly reduced, whereas $Ly6C^{lo}$ cells exhibited a 23-fold increase in comparison with WT hearts.

Inflammatory activity of leukocyte subsets may be regulated by alterations in the cell-surface expression of the signaling and decoy IL-1Rs (IL-1R1 and IL-1R2, respectively); these changes may modulate cellular responsiveness to IL-1. In vitro studies have demonstrated that in monocytes and macrophages, IL-1R1 and IL-1R2 expression is dynamically regulated by cytokines, LPS, and other bioactive mediators (24–26). Thus, we examined whether transition from the inflammatory to the proliferative phase of infarct healing is associated with changes in IL-1R expression profile. Flow cytometric analysis of cells harvested from the infarcted myocardium showed that the infarct sequentially recruits $IL\text{-}1R1^+$ and $IL\text{-}1R2^+$ cells. At the peak of the inflammatory phase (24 h of reperfusion), cells expressing IL-1R1 predominate (Fig. 2); however, their number is significantly reduced after 7 d of reperfusion, suggesting a loss of responsiveness to the effects of IL-1. Reduced numbers of $IL\text{-}1R1^+$ cells during the proliferative phase of infarct healing may reflect suppression of IL-1R1 expression, recruitment of $IL\text{-}1R1^-$ leukocyte subpopulations, or clearance of apoptotic $IL\text{-}1R1^+$ cells from the infarct. As the number of cells expressing the signaling receptor decreases, cells expressing the decoy type 2 receptor infiltrate the healing infarct. Increased numbers of $IL\text{-}1R2^+$ cells may reflect upregulation of the decoy receptor in "anti-inflammatory" macrophages or new recruitment of $IL\text{-}1R2^+$ mono-

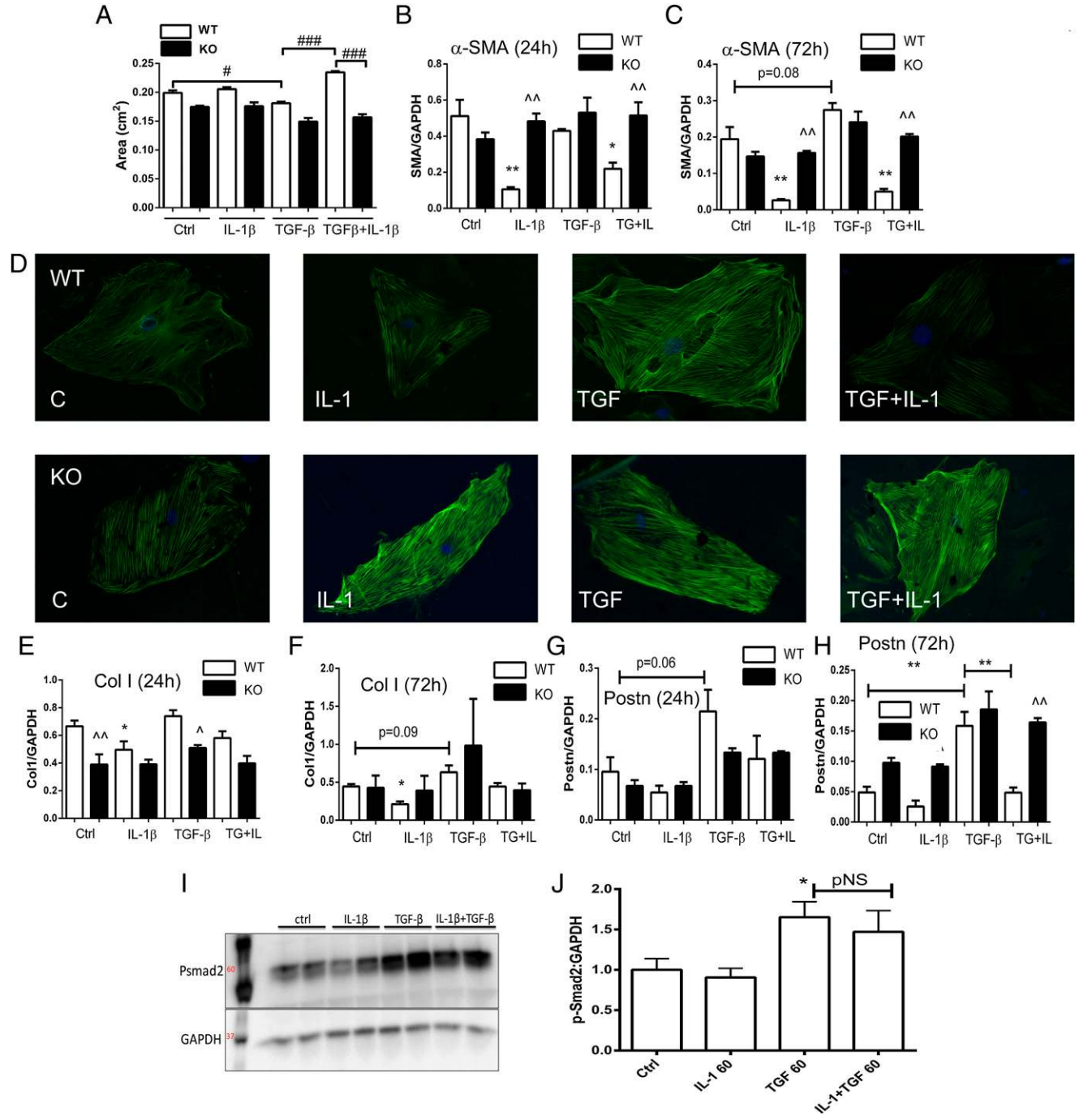

FIGURE 6. IL-1β inhibits TGF-β–induced contraction of fibroblast-populated collagen pads and attenuates α-SMA expression in an IL-1R1–dependent manner, but does not affect early Smad2 activation. (**A**) TGF-β stimulation induced contraction of collagen pads populated with WT fibroblasts ($^{\#}p < 0.05$). IL-1β abrogated the effects of TGF-β on collagen pad contraction ($^{\#\#\#}p < 0.001$). Collagen pads populated with IL-1R1 null cardiac fibroblasts had no response to IL-1 stimulation exhibiting increased contraction when compared with pads populated with WT cells. Please note that collagen pads populated with IL-1R1 null cells had enhanced baseline contraction, perhaps reflecting loss of autocrine effects of IL-1. (**B** and **C**) IL-1β attenuated α-SMA mRNA expression in control and TGF-β–stimulated cardiac fibroblasts after 24 (B) or 72 h (C) of stimulation ($^{*}p < 0.05$ versus TGF-β–stimulated, $^{**}p < 0.01$ versus C). IL-1R1 absence abrogated the inhibitory effects of IL-1β ($^{\wedge\wedge}p < 0.01$ versus corresponding WT cells). (**D**) Representative images showing α-SMA immunofluorescence support the qPCR findings (original magnification ×400). IL-1β stimulation reduced α-SMA incorporation in the cytoskeleton in control and TGF-β–stimulated fibroblasts (*upper row*). IL-1β had no effects on α-SMA immunoreactivity in IL-1R1$^{-/-}$ cells (*lower row*). (**E** and **F**) IL-1β stimulation for 24 and 72 h modestly suppressed collagen I mRNA synthesis by cardiac fibroblasts ($^{*}p < 0.05$ versus C). No significant differences in collagen I mRNA expression were noted between WT and IL-1R1 KO cells. (**G** and **H**) Expression of the matricellular protein periostin, an indicator of myofibroblast activation, was upregulated in TGF-β–stimulated fibroblasts after 24 or 72 h of stimulation. IL-1β suppressed periostin expression by TGF-β–stimulated cells after 72 h of stimulation (H). The effects of IL-1β were dependent on IL-1R1 signaling ($^{\wedge\wedge}p < 0.01$ versus corresponding WT cells). (**I** and **J**) Because Smad2/3 signaling mediates myofibroblast transdifferentiation and contractile activity, we examined whether IL-1β modulates TGF-β–induced Smad phosphorylation. Western blotting experiments demonstrated that TGF-β stimulation for 60 min increased expression of p-Smad2; however, IL-1β had no effects on Smad2 phosphorylation.

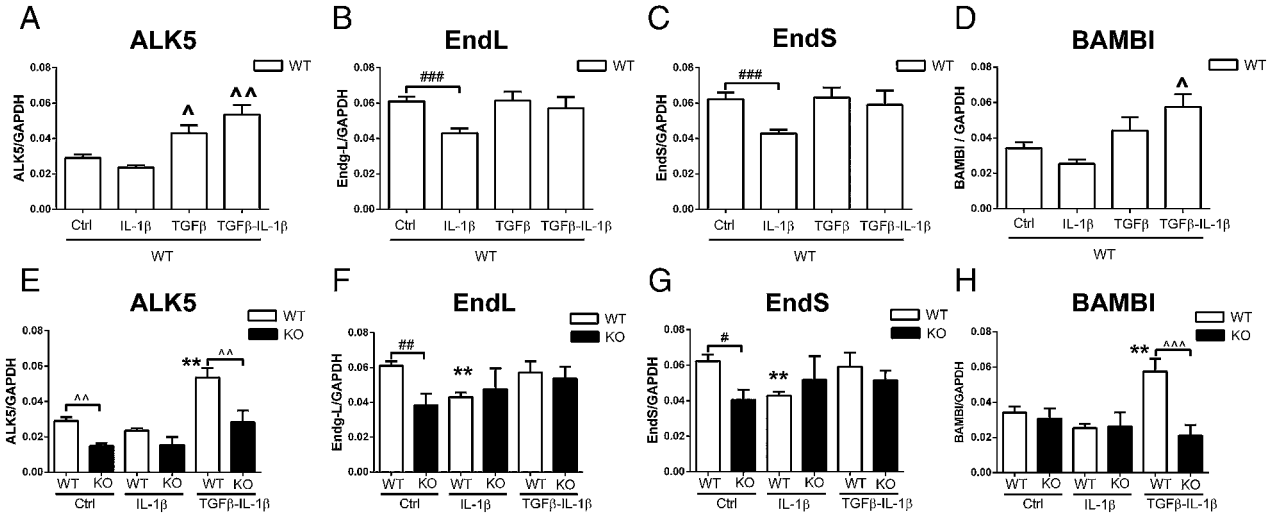

FIGURE 7. IL-1β stimulation alters the TGF-βR expression profile in cardiac fibroblasts populating collagen pads, reducing expression of endoglin and accentuating TGF-β–induced synthesis of the inhibitory receptor BAMBI. (**A**) TGF-β and TGF-β/IL-1β costimulation, but not IL-1β alone, upregulated ALK5 mRNA expression in isolated cardiac fibroblasts. (**B** and **C**) IL-1β downregulated endoglin-L (EndL) and endoglin-S (EndS) mRNA synthesis. $^{###}p < 0.001$ versus control. In contrast, TGF-β stimulation had no effects on endoglin levels. (**D**) IL-1β and TGF-β did not affect expression of BAMBI, a negative regulator of TGF-β signaling; however, costimulation with IL-1β and TGF-β significantly upregulated BAMBI mRNA levels. (**E**) IL-1R1 null cardiac fibroblasts had reduced baseline levels of ALK5 in comparison with WT cells. $^{\wedge\wedge}p < 0.01$ versus corresponding WT. (**F** and **G**) IL-1R1 null cells had reduced baseline levels of endoglins; the inhibitory effects of IL-1β on endoglin expression were abrogated in IL-1R1 null cells. BAMBI expression was comparable between WT and IL-1R1 null cardiac fibroblasts; however, the stimulatory effects of IL-1β/TGF-β on BAMBI levels were dependent on IL-1R1 signaling (**H**). $^{\wedge}p < 0.05$, $^{\#}p < 0.05$, $^{\#\#}p < 0.01$, $^{**}p < 0.01$ versus corresponding control.

cyte subpopulations. Late recruitment, or differentiation, of cells expressing the decoy receptor may serve as a mechanism for termination of IL-1 signaling in the infarcted heart.

IL-1R1 signaling mediates leukocyte infiltration in the infarcted heart

IL-1α and IL-1β signal by binding to IL-1R1, their only signaling receptor. IL-1R1 engagement leads to formation of a complex with the IL-1R accessory protein; this signaling platform sequentially recruits MyD88, IL-1R–associated kinase-1, and -4 initiating the cascade that ultimately leads to NF-κB activation and induction of a wide range of proinflammatory cytokines, chemokines, and adhesion molecules (27). In vivo, several investigations have demonstrated the essential role of IL-1R1 signaling in inflammatory processes involving many different tissues. In a model of diet-induced obesity, IL-1 signaling was found to be an essential mediator in inflammatory activation of adipose tissue macrophages (28). In bleomycin-induced lung injury, pulmonary inflammation required IL-1R1/MyD88 signaling (29); moreover, in a model of spinal cord injury, IL-1R1 or MyD88 loss resulted in markedly attenuated infiltration with proinflammatory monocytes (30). In some studies, the effects of IL-1 signaling appear to be dependent on the site of injury: IL-1R1 disruption reduced inflammatory leukocyte recruitment in a model of oral wounding but had no effects on dermal injury (31).

Does IL-1 signaling selectively mediate recruitment of proinflammatory and reparative monocytes? IL-1R1 loss markedly reduced the cellular content of reperfused myocardial infarcts; decreased cellular infiltration in animals with impaired IL-1 signaling was due to attenuated recruitment of hematopoietic cells (Table II). IL-1R1 null mice had a global reduction in leukocyte recruitment affecting both proinflammatory $Ly6C^{hi}$ and reparative $Ly6C^{lo}$ cells. These findings may suggest that IL-1 is not selectively implicated in recruitment of proinflammatory leukocytes, but has global effects on leukocyte trafficking that may be mediated through induction of adhesion molecules or through upregulation of a broad range of chemokines.

Cardiac fibroblasts as cellular targets of IL-1 in the infarcted myocardium

Fibroblasts are the predominant noncardiomyocyte population in the adult human myocardium (32). In addition to their role as matrix-synthetic cells, fibroblasts may also serve as sentinel cells that sense microenvironmental changes and play an important role in initiation of inflammatory responses (33, 34). Following myocardial ischemia, cardiac fibroblasts are capable of activating the inflammasome, triggering IL-1–driven inflammation (35), and may be important sources of cytokines and chemokines. Our experiments demonstrate that the proinflammatory actions of IL-1R1 signaling are not limited to leukocytes, but also involve fibroblasts. $CD11b^{-}$ cells harvested from the infarcted heart exhibited significant upregulation of proinflammatory genes; loss of IL-1R1 attenuated inflammatory gene expression by nonmyeloid cells (Fig. 4). Myeloid and $CD11b^{-}$ cells were harvested from whole hearts; thus, our experiments do not provide information on the potentially distinct cellular phenotypes in the infarcted and noninfarcted remodeling myocardium. Because during the inflammatory phase of infarct healing, cytokine upregulation is primarily localized in the infarcted area, the effects of IL-1R1 loss may

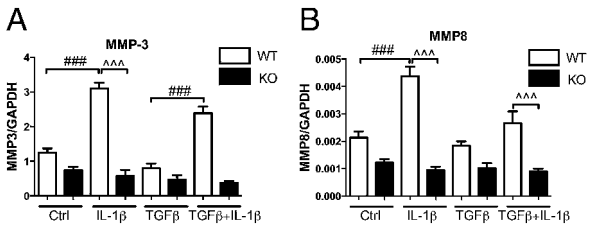

FIGURE 8. IL-1 accentuates fibroblast-derived MMP expression in an IL-1R1–dependent manner. IL-1β stimulation induced MMP-3 (**A**) and MMP-8 synthesis (**B**) in fibroblasts populating collagen pads ($^{###}p < 0.001$ versus control). In contrast, TGF-β had no effects on MMP synthesis. The stimulatory effects of IL-1β on MMP-3 and MMP-8 expression were abrogated in IL-1R1 null cells ($^{\wedge\wedge\wedge}p < 0.001$ versus corresponding WT cells).

primarily reflect IL-1 actions on cells infiltrating the infarct. In addition to its effects in promoting proinflammatory signaling, IL-1 also induced MMP expression in cardiac fibroblasts, thus stimulating matrix-degrading activity (Fig. 8).

Myofibroblast transdifferentiation is the hallmark of the proliferative phase of cardiac repair (36); differentiated myofibroblasts are the main matrix-producing cells in the infarcted heart (37). Activation of TGF-β signaling provides a key signal for acquisition of myofibroblast phenotype; matrix alterations such as deposition of the ED-A isoform of cellular fibronectin and induction of matricellular proteins also contribute to the phenotypic transition of fibroblasts into myofibroblasts. However, despite the early presence of bioactive TGF-β in the infarcted myocardium within the first 3 h of reperfusion (38), myofibroblast transdifferentiation in healing infarcts is delayed until proinflammatory signaling has been suppressed and the local environment can support a large population of matrix-secreting cells (39). To our knowledge, our findings demonstrate for the first time that IL-1 inhibits TGF-β–induced contraction of fibroblast-populated collagen pads, suppressing α-SMA and periostin synthesis, attenuating functional and molecular responses that directly reflect myofibroblast transdifferentiation (Fig. 6). Thus, in addition to its proinflammatory actions, IL-1 signaling may also serve to prevent premature conversion of fibroblasts into myofibroblasts during the inflammatory phase of cardiac repair, at a time point when the infarct environment may be hostile to reparative and contractile cells. Suppression of IL-1 expression and termination of IL-1 signaling during the proliferative phase of infarct healing may allow unopposed actions of TGF-β on cardiac fibroblasts mediating myofibroblast transdifferentiation and scar contraction.

What is the mechanism of IL-1–mediated inhibition of the TGF-β response?

IL-1–mediated suppression of TGF-β signaling in cardiac fibroblasts is not due to direct effects on TGF-induced Smad2 phosphorylation (Fig. 6B, 6C). The effects of IL-1β may reflect alterations on the TGF-βR expression profile in cardiac fibroblasts (Fig. 7). IL-1–induced downregulation of the TGF-β coreceptor endoglin, a critical component of profibrotic TGF-β signaling, may be an important mechanism in mediating the inhibitory effects of IL-1 on TGF-β signaling. Expression of the TGF-β coreceptor endoglin is increased in failing hearts and has been linked with the development of cardiac fibrosis (40). IL-1 may also stimulate molecular signals that negatively regulate the TGF-β response. When added to TGF-β, IL-1β increased fibroblast expression of the BAMBI, a transmembrane molecule that decreases formation of the functional TβRI/TβRII complex, thus negatively regulating the TGF-β response (41). BAMBI overexpression in fibroblasts has been reported to enhance TGF-β–mediated effects (42).

Implications for the use of anti–IL-1 approaches in patients with myocardial infarction

Because loss of IL-1 signaling attenuates adverse postinfarction remodeling (7) and IL-1 exerts proapoptotic effects on cardiomyocytes (8), anti–IL-1 strategies have been proposed as therapy for patients with acute myocardial infarction. In a small pilot study, administration of anakinra was safe and attenuated dilative remodeling after myocardial infarction. These promising early results generate optimism regarding the potential effectiveness of IL-1 inhibition in preventing development of postinfarction heart failure. Our findings suggest that the protective effects of IL-1 inhibition may be because of decreased recruitment of proinflammatory leukocytes and reduced activation of inflammatory and matrix-degrading properties in cardiac fibroblasts. However, our experiments also suggest caution regarding effects of disturbed IL-1 signaling on orchestration of the reparative response. Anti–IL-1 treatment may result in impaired recruitment of reparative monocyte subsets and in premature acquisition of the myofibroblast phenotype, thus causing perturbations in the reparative process. Moreover, disruption of IL-1 signaling may cause loss of unrecognized cytoprotective signals on ischemic cardiomyocytes. Dissection of the cell biological actions of IL-1 signaling is needed to optimally guide design of therapeutic approaches in the infarcted and remodeling heart.

Acknowledgments

We thank the Albert Einstein College of Medicine Flow cytometry core facility for expert assistance.

Disclosures

The authors have no financial conflicts of interest.

References

1. Dinarello, C. A. 2011. A clinical perspective of IL-1β as the gatekeeper of inflammation. *Eur. J. Immunol.* 41: 1203–1217.
2. Dinarello, C. A., A. Simon, and J. W. van der Meer. 2012. Treating inflammation by blocking interleukin-1 in a broad spectrum of diseases. *Nat. Rev. Drug Discov.* 11: 633–652.
3. Bujak, M., and N. G. Frangogiannis. 2009. The role of IL-1 in the pathogenesis of heart disease. *Arch. Immunol. Ther. Exp. (Warsz.)* 57: 165–176.
4. Denes, A., C. Drake, J. Stordy, J. Chamberlain, B. W. McColl, H. Gram, D. Crossman, S. Francis, S. M. Allan, and N. J. Rothwell. 2012. Interleukin-1 mediates neuroinflammatory changes associated with diet-induced atherosclerosis. *J Am Heart Assoc* 1: e002006.
5. Ridker, P. M., T. Thuren, A. Zalewski, and P. Libby. 2011. Interleukin-1β inhibition and the prevention of recurrent cardiovascular events: rationale and design of the Canakinumab Anti-inflammatory Thrombosis Outcomes Study (CANTOS). *Am. Heart J.* 162: 597–605.
6. Dewald, O., G. Ren, G. D. Duerr, M. Zoerlein, C. Klemm, C. Gersch, S. Tincey, L. H. Michael, M. L. Entman, and N. G. Frangogiannis. 2004. Of mice and dogs: species-specific differences in the inflammatory response following myocardial infarction. *Am. J. Pathol.* 164: 665–677.
7. Bujak, M., M. Dobaczewski, K. Chatila, L. H. Mendoza, N. Li, A. Reddy, and N. G. Frangogiannis. 2008. Interleukin-1 receptor type I signaling critically regulates infarct healing and cardiac remodeling. *Am. J. Pathol.* 173: 57–67.
8. Abbate, A., F. N. Salloum, E. Vecile, A. Das, N. N. Hoke, S. Straino, G. G. Biondi-Zoccai, J. E. Houser, I. Z. Qureshi, E. D. Ownby, et al. 2008. Anakinra, a recombinant human interleukin-1 receptor antagonist, inhibits apoptosis in experimental acute myocardial infarction. *Circulation* 117: 2670–2683.
9. Haudek, S. B., G. E. Taffet, M. D. Schneider, and D. L. Mann. 2007. TNF provokes cardiomyocyte apoptosis and cardiac remodeling through activation of multiple cell death pathways. *J. Clin. Invest.* 117: 2692–2701.
10. Schulz, R., D. L. Panas, R. Catena, S. Moncada, P. M. Olley, and G. D. Lopaschuk. 1995. The role of nitric oxide in cardiac depression induced by interleukin-1 beta and tumour necrosis factor-alpha. *Br. J. Pharmacol.* 114: 27–34.
11. Li, Y. Y., Y. Q. Feng, T. Kadokami, C. F. McTiernan, R. Draviam, S. C. Watkins, and A. M. Feldman. 2000. Myocardial extracellular matrix remodeling in transgenic mice overexpressing tumor necrosis factor alpha can be modulated by anti-tumor necrosis factor alpha therapy. *Proc. Natl. Acad. Sci. USA* 97: 12746–12751.
12. Kurrelmeyer, K. M., L. H. Michael, G. Baumgarten, G. E. Taffet, J. J. Peschon, N. Sivasubramanian, M. L. Entman, and D. L. Mann. 2000. Endogenous tumor necrosis factor protects the adult cardiac myocyte against ischemic-induced apoptosis in a murine model of acute myocardial infarction. *Proc. Natl. Acad. Sci. USA* 97: 5456–5461.
13. Hamid, T., Y. Gu, R. V. Ortines, C. Bhattacharya, G. Wang, Y. T. Xuan, and S. D. Prabhu. 2009. Divergent tumor necrosis factor receptor-related remodeling responses in heart failure: role of nuclear factor-kappaB and inflammatory activation. *Circulation* 119: 1386–1397.
14. Mann, D. L., J. J. McMurray, M. Packer, K. Swedberg, J. S. Borer, W. S. Colucci, J. Djian, H. Drexler, A. Feldman, L. Kober, et al. 2004. Targeted anticytokine therapy in patients with chronic heart failure: results of the Randomized Etanercept Worldwide Evaluation (RENEWAL). *Circulation* 109: 1594–1602.
15. Abbate, A., M. C. Kontos, J. D. Grizzard, G. G. Biondi-Zoccai, B. W. Van Tassell, R. Robati, L. M. Roach, R. A. Arena, C. S. Roberts, A. Varma, et al; VCU-ART Investigators. 2010. Interleukin-1 blockade with anakinra to prevent adverse cardiac remodeling after acute myocardial infarction (Virginia Commonwealth University Anakinra Remodeling Trial [VCU-ART] Pilot study). *Am J Cardiol.* 105: 1371–1377.e1.
16. Labow, M., D. Shuster, M. Zetterstrom, P. Nunes, R. Terry, E. B. Cullinan, T. Bartfai, C. Solorzano, L. L. Moldawer, R. Chizzonite, and K. W. McIntyre. 1997. Absence of IL-1 signaling and reduced inflammatory response in IL-1 type I receptor-deficient mice. *J. Immunol.* 159: 2452–2461.
17. Dobaczewski, M., Y. Xia, M. Bujak, C. Gonzalez-Quesada, and N. G. Frangogiannis. 2010. CCR5 signaling suppresses inflammation and

reduces adverse remodeling of the infarcted heart, mediating recruitment of regulatory T cells. *Am. J. Pathol.* 176: 2177–2187.
18. Bujak, M., M. Dobaczewski, C. Gonzalez-Quesada, Y. Xia, T. Leucker, P. Zymek, V. Veeranna, A. M. Tager, A. D. Luster, and N. G. Frangogiannis. 2009. Induction of the CXC chemokine interferon-gamma-inducible protein 10 regulates the reparative response following myocardial infarction. *Circ. Res.* 105: 973–983.
19. Dobaczewski, M., M. Bujak, N. Li, C. Gonzalez-Quesada, L. H. Mendoza, X. F. Wang, and N. G. Frangogiannis. 2010. Smad3 signaling critically regulates fibroblast phenotype and function in healing myocardial infarction. *Circ. Res.* 107: 418–428.
20. Nahrendorf, M., F. K. Swirski, E. Aikawa, L. Stangenberg, T. Wurdinger, J. L. Figueiredo, P. Libby, R. Weissleder, and M. J. Pittet. 2007. The healing myocardium sequentially mobilizes two monocyte subsets with divergent and complementary functions. *J. Exp. Med.* 204: 3037–3047.
21. Frangogiannis, N. G. 2012. Matricellular proteins in cardiac adaptation and disease. *Physiol. Rev.* 92: 635–688.
22. Oka, T., J. Xu, R. A. Kaiser, J. Melendez, M. Hambleton, M. A. Sargent, A. Lorts, E. W. Brunskill, G. W. Dorn, II, S. J. Conway, et al. 2007. Genetic manipulation of periostin expression reveals a role in cardiac hypertrophy and ventricular remodeling. *Circ. Res.* 101: 313–321.
23. Dewald, O., P. Zymek, K. Winkelmann, A. Koerting, G. Ren, T. Abou-Khamis, L. H. Michael, B. J. Rollins, M. L. Entman, and N. G. Frangogiannis. 2005. CCL2/Monocyte Chemoattractant Protein-1 regulates inflammatory responses critical to healing myocardial infarcts. *Circ. Res.* 96: 881–889.
24. Colotta, F., F. Re, M. Muzio, R. Bertini, N. Polentarutti, M. Sironi, J. G. Giri, S. K. Dower, J. E. Sims, and A. Mantovani. 1993. Interleukin-1 type II receptor: a decoy target for IL-1 that is regulated by IL-4. *Science* 261: 472–475.
25. Colotta, F., S. K. Dower, J. E. Sims, and A. Mantovani. 1994. The type II 'decoy' receptor: a novel regulatory pathway for interleukin 1. *Immunol. Today* 15: 562–566.
26. Saccani, S., N. Polentarutti, G. Penton-Rol, J. E. Sims, and A. Mantovani. 1998. Divergent effects of LPS on expression of IL-1 receptor family members in mononuclear phagocytes in vitro and in vivo. *Cytokine* 10: 773–780.
27. O'Neill, L. A. 2008. The interleukin-1 receptor/Toll-like receptor superfamily: 10 years of progress. *Immunol. Rev.* 226: 10–18.
28. McGillicuddy, F. C., K. A. Harford, C. M. Reynolds, E. Oliver, M. Claessens, K. H. Mills, and H. M. Roche. 2011. Lack of interleukin-1 receptor I (IL-1RI) protects mice from high-fat diet-induced adipose tissue inflammation coincident with improved glucose homeostasis. *Diabetes* 60: 1688–1698.
29. Gasse, P., C. Mary, I. Guenon, N. Noulin, S. Charron, S. Schnyder-Candrian, B. Schnyder, S. Akira, V. F. Quesniaux, V. Lagente, et al. 2007. IL-1R1/MyD88 signaling and the inflammasome are essential in pulmonary inflammation and fibrosis in mice. *J. Clin. Invest.* 117: 3786–3799.
30. Pineau, I., L. Sun, D. Bastien, and S. Lacroix. 2010. Astrocytes initiate inflammation in the injured mouse spinal cord by promoting the entry of neutrophils and inflammatory monocytes in an IL-1 receptor/MyD88-dependent fashion. *Brain Behav. Immun.* 24: 540–553.
31. Graves, D. T., N. Nooh, T. Gillen, M. Davey, S. Patel, D. Cottrell, and S. Amar. 2001. IL-1 plays a critical role in oral, but not dermal, wound healing. *J. Immunol.* 167: 5316–5320.
32. Souders, C. A., S. L. Bowers, and T. A. Baudino. 2009. Cardiac fibroblast: the renaissance cell. *Circ. Res.* 105: 1164–1176.
33. Smith, R. S., T. J. Smith, T. M. Blieden, and R. P. Phipps. 1997. Fibroblasts as sentinel cells. Synthesis of chemokines and regulation of inflammation. *Am. J. Pathol.* 151: 317–322.
34. Chen, W., and N. G. Frangogiannis. 2013. Fibroblasts in post-infarction inflammation and cardiac repair. *Biochim. Biophys. Acta* 1833: 945–953.
35. Kawaguchi, M., M. Takahashi, T. Hata, Y. Kashima, F. Usui, H. Morimoto, A. Izawa, Y. Takahashi, J. Masumoto, J. Koyama, et al. 2011. Inflammasome activation of cardiac fibroblasts is essential for myocardial ischemia/reperfusion injury. *Circulation* 123: 594–604.
36. Willems, I. E., M. G. Havenith, J. G. De Mey, and M. J. Daemen. 1994. The alpha-smooth muscle actin-positive cells in healing human myocardial scars. *Am. J. Pathol.* 145: 868–875.
37. Cleutjens, J. P., M. J. Verluyten, J. F. Smiths, and M. J. Daemen. 1995. Collagen remodeling after myocardial infarction in the rat heart. *Am. J. Pathol.* 147: 325–338.
38. Birdsall, H. H., D. M. Green, J. Trial, K. A. Youker, A. R. Burns, C. R. MacKay, G. J. LaRosa, H. K. Hawkins, C. W. Smith, L. H. Michael, et al. 1997. Complement C5a, TGF-beta 1, and MCP-1, in sequence, induce migration of monocytes into ischemic canine myocardium within the first one to five hours after reperfusion. *Circulation* 95: 684–692.
39. Frangogiannis, N. G., L. H. Michael, and M. L. Entman. 2000. Myofibroblasts in reperfused myocardial infarcts express the embryonic form of smooth muscle myosin heavy chain (SMemb). *Cardiovasc. Res.* 48: 89–100.
40. Kapur, N. K., S. Wilson, A. A. Yunis, X. Qiao, E. Mackey, V. Paruchuri, C. Baker, M. J. Aronovitz, S. A. Karumanchi, M. Letarte, et al. 2012. Reduced endoglin activity limits cardiac fibrosis and improves survival in heart failure. *Circulation* 125: 2728–2738.
41. Onichtchouk, D., Y. G. Chen, R. Dosch, V. Gawantka, H. Delius, J. Massagué, and C. Niehrs. 1999. Silencing of TGF-beta signalling by the pseudoreceptor BAMBI. *Nature* 401: 480–485.
42. Villar, A. V., R. García, M. Llano, M. Cobo, D. Merino, A. Lantero, M. Tramullas, J. M. Hurlé, M. A. Hurlé, and J. F. Nistal. 2013. BAMBI (BMP and activin membrane-bound inhibitor) protects the murine heart from pressure-overload biomechanical stress by restraining TGF-β signaling. *Biochim. Biophys. Acta* 1832: 323–335.